Rapid communication

Devarajan Kaliyannan*

Nonlinear dynamics and parametric study of snap through electromagnetic vibration energy harvester using multi-term harmonic balance method

https://doi.org/10.1515/ehs-2020-0004
Received December 6, 2020; accepted March 3, 2021;
published online April 12, 2021

Abstract: Vibration energy harvester (VEH) has proven to be a favorable potential technique to supply continuous energy from ambient vibrations and its performance is greatly influenced by the design of potential structures. A snap-through mechanism is used in an electromagnetic energy harvester to improve its effectiveness. It mainly comprises of three springs that are configured so that the potential energy of the system has two stable equilibrium points. In this work, a harmonically base excited snap-through electromagnetic vibration energy harvester is investigated by analytical and semi-analytical method. The approximate analytical outcomes are qualitatively and quantitatively supported by semi-analytical method using multi-term harmonic balance method (MHBM).The bifurcation diagram of response current shows that snap-through electromagnetic vibration energy harvesters exhibits periodic intrawell, interwell and chaotic motion when the system parameters are varied. The influence of system parameters on the response of snap-through electromagnetic vibration energy harvester are examined. Nonlinearity produced by the snap-through oscillator improves energy harvesting so that the snap-through electromagnetic energy harvester can outperform the linear energy harvester in the similar size under harmonic excitation. A fitness function was formulated and optimization of the selected parameters was done using genetic algorithm. The parametric optimization leads to a considerable improvement in the harvested current from the system.

***Corresponding author: Devarajan Kaliyannan**, Department of Mechanical Engineering, Amrita School of Engineering, Amrita Vishwa Vidyapeetham, Coimbatore, India,
E-mail: k_devarajan@cb.amrita.edu. https://orcid.org/0000-0002-4983-8184

Keywords: bifurcation; electromagnetic transduction; genetic algorithm; multi-term harmonic balance method; optimization; snap-through energy harvester.

Introduction

VEHs are scalable electro-mechanical devices that are used to power low powered wireless devices and sensors (Elvin and Erturk 2013; Erturk and Inman 2011a; Priya and Inman 2009). Ali and Adhikari (2013) proposed a dynamic vibration absorber combined with piezoelectric transducer for both vibration absorption and energy harvesting simultaneously. The dynamics, vibration absorption and energy harvesting abilities of combined nonlinear vibration absorber with energy harvester system was also investigated (Santhosh and Das 2016; Raj and Santhosh 2019; Raj and Santhosh 2020). Many review papers are available which dealt the importance of nonlinear approach in performance improvement of vibration energy harvesters (Daqaq et al. 2014; Tran, Ghayesh, and Arjomandi 2018; Yildirim et al. 2017). Priya et al. (Zhou et al. 2017) provided the state-of-the-art in microscale piezoelectric energy harvesting, summarizing key metrics such as power density and bandwidth of reported structures at low frequency input. Rantz and Roundy (2017) provided an additional insight into the prevalence and characteristics of vibrations commonly encountered in the environment and application to nonlinear vibration energy harvesters.

Bistable energy harvesters received more attention due to its ability to generate high power when the device undergoes from one stable state to another stable state, which could cause large amplitude motion and drastically increase power generation (Harne and Kon-Well 2017). Harne and Wang (2013) provided detailed review on vibration energy harvesting via bistable systems. Erturk and Inman (2011b) conducted an experimental and theoretical investigations on non-resonant bistable

piezomagnetoelastic energy harvester over a wide range of excitation frequencies.

Snap-through mechanisms are the most common types of bistable system. The smooth and discontinuous (SD) oscillator is actually a bistable system whose dynamics was well studied by many researchers and well recorded in the literature (Cao et al. 2006, 2008; Santhosh, Padmanabhan, and Narayanan 2014; Tian, Cao, and Yang 2010). Jiang and Chen (2014) used the snap-through oscillator as a vibration energy harvester using piezoelectric transduction mechanism. Yang and Cao (2020) presented a novel multi-stable electromagnetic transduction energy harvesting system by adjusting the geometric parameters of linear springs and proved that the multi-stable energy harvesting system composed of a nonlinear restoring force can significantly improve the efficiency of the energy converter under low external excitation. Ramlan et al. (2010) showed that more power is harvested by the nonlinear snap-through bistable energy harvester for the excitation frequency much less than the natural frequency of the system. Jiang and Chen (2016) employed the snap-through mechanism to harvest energy through electromagnetic transduction mechanism from external Gaussian white noise and parametric excitation and revealed that snap-through energy harvesters outperform the linear vibration energy harvester. Yang, Liu, and Cao (2018) investigated the efficiency of electromagnetic vibration energy harvester of the snap-through oscillator and concluded that they perform better than linear one when subjected to harmonic and stochastic excitation.

Although the snap-through mechanism for vibration energy harvesting is well studied, the steady state displacement and current response of the system using analytical and semi-analytical techniques is limited. The present article describes an analytical and semi-analytical analyses of snap-through electromagnetic vibration energy harvester under harmonic excitation. Bifurcation analysis is performed as excitation frequency as parameters for different values of nonlinear geometric coefficient using numerical integration. In order to understand the energy harvesting performance in detail, the effects of the system parameters on the response of the system are studied by using semi-analytical method. The energy harvesting performance of snap-through electromagnetic energy harvester and linear harvester with similar size is compared. The optmization processes also carried out to find the optimal parameters to enhance the performance of energy harvester.

The work of this paper is organized as follows. In Section 2, the equations of motion for a snap-through electromagnetic vibration energy harvester is derived. In Sections 3 and 4, analytical and semi-analytical analysis are performed to find out the response of the system. Comparison between harmonic balance method and semi-analytical (MHBM) is presented in Section 5. Bifurcation analysis of snap-through energy harvester is conducted in Section 6. Parametric study is explained in Section 7. Section 8 compares the produced displacement and current response of the snap-through electromagnetic energy harvester and the linear electromagnetic energy harvester of the similar size. Section 9 discuss the optimized results of the energy harvester. Finally, Section 10 is an overview of the conclusion.

Mathematical modelling and equation of motion

Figure 1 shows a physical model of an electromagnetic energy harvester based on a snap-through mechanism. The model consists of a mass M forced to move in the vertical direction. The system has a vertical spring K_v in addition to two horizontal springs with stiffness K_h of free length L and damper C. $X(t)$ is the displacement of the mass from the mean position. Electromagnetic transduction mechanism is attached with the snap-through oscillator and is characterized by the parameters, the electric current output $\bar{I}$, resistance of the coil R_C, inductance L_i and effective coil length L_c. The electromagnetic transduction mechanism is connected to external resistors R and the magnetic field B is provided by a permanent magnet which is fixed to the enclosure. The distance between the two sliders is denoted as $2l$. The base of the system is excited with a harmonic input $Y(t)$.

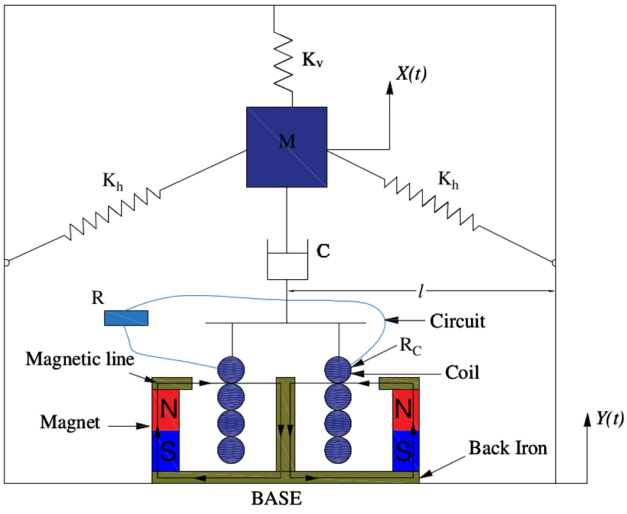

Figure 1: Model of snap-through oscillator with electromagnetic transduction mechanism.

The equations of motion for the base excited system considering electromagnetic transduction mechanism is given by

$$M\ddot{X} + C\dot{X} + K_v X + 2K_h X\left(1 - \frac{L}{\sqrt{X^2 + l^2}}\right) + BL_c\bar{I} = -M\ddot{Y} \quad (1)$$

$$L_i\dot{\bar{I}} + (R + R_c)\bar{I} = BL_c\dot{X} \quad (2)$$

The equations of motion are non-dimensionalized by considering the following non-dimensional parameters,

$$x = \frac{X}{L}, \quad y = \frac{Y}{L}, \quad 2\zeta = \frac{C}{M\omega_1}, \quad \omega_1^2 = \frac{K_v}{M},$$

$$\omega_2^2 = \frac{2K_h}{M}, \quad r = \frac{\omega_2^2}{\omega_1^2}, \quad \alpha = \frac{l}{L} \quad \theta = \frac{BL_c}{M\omega_1^2}, \quad I = \frac{\bar{I}}{L}, \quad f = \frac{F}{ML\omega_1^2},$$

$$\tau = \omega_1 t, \quad \Omega = \frac{\omega}{\omega_1}, \quad \lambda = \frac{R + R_c}{L_i}, \quad \mu = \frac{BL_c\omega_1}{L_i}$$

where ω_1 is the natural frequency of the associated single degree of freedom linear system, ζ is the damping factor, θ is the linear dimensionless electro-mechanical coupling coefficient in the mechanical equation, α is the non-dimensional geometrical coefficient, r is the non-dimensional nonlinear stiffness coefficient, λ is the ratio between the resistance and inductance which is constants of the harvester and μ is the electromagnetic coupling term in the current equation. The equations of motion are represented in terms of the non-dimensional time τ with the non-dimensional parameters explained above as

$$x'' + 2\zeta x' + x + rx\left(1 - \frac{1}{\sqrt{x^2 + \alpha^2}}\right) + \theta I = f\cos(\Omega\tau) \quad (3)$$

$$I' + \lambda I - \mu x' = 0 \quad (4)$$

The number of primes represent the order of differentiation with respect to non-dimensional time τ. The fixed points are

$$x_1^* = 0, \quad x_{2,3}^* = \pm\sqrt{\frac{-2r\alpha^2 - r^2\alpha^2 + r^2 - \alpha^2}{1 + r}} \quad (5)$$

The analytical expressions for forcing, potential and stiffness functions are given below.

$$F(x) = x + rx\left(1 - \frac{1}{\sqrt{x^2 + \alpha^2}}\right) \quad (6)$$

$$V(x) = \frac{1}{2}x^2 + r\left(-\sqrt{x^2 + \alpha^2} + \frac{1}{2}x^2\right) + r\alpha \quad (7)$$

$$K(x) = 1 + r\left(1 - \frac{1}{\sqrt{x^2 + \alpha^2}}\right) + \frac{rx^2}{(x^2 + \alpha^2)^{1.5}} \quad (8)$$

The variation of the restoring force and the potential function for different values of α is shown in Figure 2(a) and (b). It is observed that the system starts exhibits monostable behaviour when α is greater than 0.49.

Analytical analysis by harmonic balance method

The governing equation of snap-through electromagnetic energy harvester is expanded by binomial form about α and neglecting higher order term, the governing equation can be written as

$$x'' + 2\zeta x' + x + rx - \frac{rx}{\alpha} + \frac{1}{2}\frac{rx^3}{\alpha^3} + \theta I = f\cos(\Omega\tau) \quad (9)$$

$$I' + \lambda I - \mu x' = 0 \quad (10)$$

Harmonic balance method have been widely applied to investigate the nonlinear dynamics and performance analysis of nonlinear vibration energy harvesters. In order to analyze the response characteristics of the snap-through electromagnetic energy harvester, the steady response displacement and current of the system are assumed as follows,

$$x(t) = A\cos(\Omega t) + B\sin(\Omega t) \quad (11)$$

$$I(t) = P\cos(\Omega t) + Q\sin(\Omega t) \quad (12)$$

Substituting Eqs. (11) and (12) into Eq. (10) and balancing the terms multiplied by $\sin(\Omega t)$ and $\cos(\Omega t)$, the following equations are obtained:

$$Q\Omega - \mu B\Omega + \lambda P = 0 \quad (13)$$

$$-P\Omega + \mu A\Omega + Q\lambda = 0 \quad (14)$$

Solving the two equations one can obtain

$$P = \frac{\mu(A\Omega + B\Omega)\Omega}{\Omega^2 + \lambda^2} \quad Q = -\frac{\mu(-B\Omega + A\Omega)\Omega}{\Omega^2 + \lambda^2} \quad (15)$$

Substituting Eqs. (11) and (12) into Eq. (9) and balancing the terms multiplied by $\sin(\Omega t)$ and $\cos(\Omega t)$, we obtain

$$8\alpha^3 Ar - 8\alpha^3 A\Omega^2 + 8\alpha^3 A + 16\alpha^3\zeta\Omega B + 8\alpha^3 P\theta$$
$$-8r\alpha^2 A + 3ArB^2 + 3A^3 r = 8f\alpha^3 \quad (16)$$

$$8\alpha^3 Br - 8\alpha^3 B\Omega^2 + 8\alpha^3 B - 16\alpha^3\zeta\Omega A + 8\alpha^3 Q\theta$$
$$-8r\alpha^2 B + 3BrA^2 + 3B^3 r = 0 \quad (17)$$

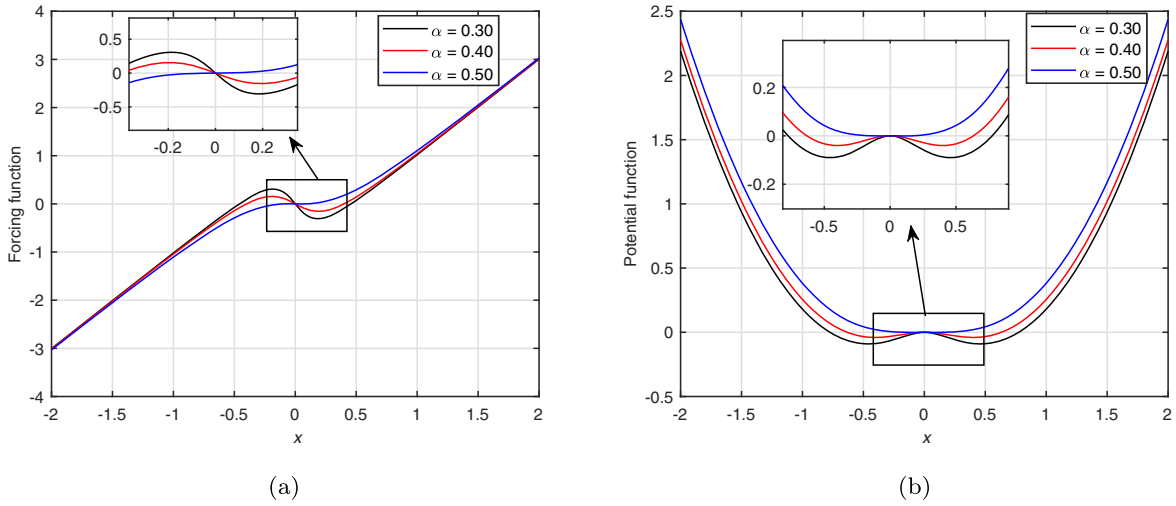

Figure 2: Variation of (a) forcing and (b) potential function of snap-through electromagnetic energy harvester for different values of α when $r = 1.0$.

Substituting Eq. (15) into Eqs. (16) and (17), the following equations are obtained

$$(8r\alpha^3 - 8\alpha^3\Omega^2 + 8\alpha^3 - 8r\alpha^2 + S\Omega + 3r\alpha^2)A + (S\lambda + 16\alpha^3\zeta\Omega)B = 8f\alpha^3 \quad (18)$$

$$(8r\alpha^3 - 8\alpha^3\Omega^2 + 8\alpha^3 - 8r\alpha^2 + S\Omega + 3r\alpha^2)B - (S\lambda + 16\alpha^3\zeta\Omega)A = 0 \quad (19)$$

where $S = \frac{8\theta\mu\Omega\alpha^3}{\Omega^2+\lambda^2}$. Based on the above two equations, the frequency response function of the steady-state displacement is expressed as

$$\left(8r\alpha^3 - 8\alpha^3\,\Omega^2 + 8\alpha^3 - 8r\alpha^2 + \frac{8\alpha^3\theta\mu\Omega^2}{\Omega^2+\lambda^2} + 3r\alpha^2\right)^2 a^2 + \left(\frac{\alpha^3 8\theta\mu\Omega\lambda}{\Omega^2+\lambda^2} + 16\alpha^3\zeta\Omega\right)^2 a^2 = 64f^2\alpha^6 \quad (20)$$

where $a = \sqrt{A^2 + B^2}$ is the displacement amplitude of the energy harvester. Also, the relationship between current and displacement can be obtained from

$$I^2 = P^2 + Q^2 = \frac{\mu^2\,\Omega^2\left(A^2 + B^2\right)}{\Omega^2 + \lambda^2} = \frac{\mu^2\,\Omega^2\,a^2}{\Omega^2 + \lambda^2} \quad (21)$$

Substituting Eq. (21) into Eq. (20), we get the frequency response function of the steady-state current of the snap-through electromagnetic energy harvester.

Semi-analytical method: multi-term harmonic balance method

Numerical solution takes more time to generate steady-state response for lightly damped systems. Multi-term harmonic balance method (MHBM) is a numeric-analytical method developed by Santhosh, Padmanabhan, and Narayanan (2014) which can be used for a harmonically exciting system to obtain the steady-state periodic solutions and it is also applicable for highly non-linear systems. The primary procedure of MHBM is explained as follows:

$$M\ddot{X} + C\dot{X} + KX + F_{nl}\left(X, \dot{X}, \ddot{X}, \alpha\right) = F(t) \quad (22)$$

where M is NXN mass matrix, C is NXN mass damping matrix, K is NXN stiffness matrix, F_{nl} is the nonlinear function vector, X is the $NX1$ displacement vector, $\dot{X}$ is the $NX1$ velocity vector, $\ddot{X}$ is the $NX1$ acceleration vector, $F(t)$ is the $NX1$ external vector and α is a system parameter. The non-dimensional equation of motion as follows

$$\omega^2 M\ddot{X} + \omega C\dot{X} + KX + F_{nl}\left(X, \dot{X}, \ddot{X}, \alpha\right) = F(\tau) \quad (23)$$

The output of the system in particularly displacement, velocity and acceleration are stated as a form of Fourier series

$$X(\tau) = A_0 + \sum_{i=1}^{n}\left(A_i\cos(i\tau) + B_i\sin(i\tau)\right) \quad (24)$$

$$\dot{X}(\tau) = \sum_{i=1}^{n} (- iA_i \sin(i\tau) + iB_i \cos(i\tau)) \tag{25}$$

$$\ddot{X}(\tau) = \sum_{i=1}^{n} \left(- i^2 A_i \cos(i\tau) - i^2 B_i \sin(i\tau)\right) \tag{26}$$

Where the Fourier coefficients are A_0, A_i, B_i respectively. n is total number of harmonics. The Fourier series of the excitation vector is also can be expressed as

$$F(\tau) = F_0 + \sum_{i=1}^{n} (F_{ci} \cos(i\tau) + F_{si} \sin(i\tau)) \tag{27}$$

where F_0, F_{ci} and F_{si} are the Fourier coefficients. In the next step, the time interval 0 to 2π is divided into p time points. The response and its derivatives are evaluated in the interval as

$$X = \Gamma Q \tag{28}$$

$$\dot{X} = \dot{\Gamma} Q \tag{29}$$

$$\ddot{X} = \ddot{\Gamma} Q \tag{30}$$

where Q is the Fourier coefficient vector. The structure of Γ matrix is given below. The matrices Γ and its derivatives are need to be evaluated only once and can be saved for further computation.

$$\Gamma = \begin{bmatrix} 1 & \cos(t_0) & \sin(t_0) & \dots & \dots & \cos(nt_0) & \sin(nt_0) \\ 1 & \cos(t_1) & \sin(t_1) & \dots & \dots & \cos(nt_1) & \sin(nt_1) \\ \dots & \dots & \dots & \dots & \dots & \dots & \dots \\ \vdots & \vdots & \vdots & \vdots & \vdots & \vdots & \vdots \\ 1 & \cos(t_p) & \sin(t_p) & \dots & \dots & \cos(nt_p) & \sin(nt_p) \end{bmatrix}$$

In a similar way, the Fourier coefficients correspond to the nonlinear function F_{nl} and external excitation F_{ext} can be obtained as

$$G = \Gamma^{-1} F_{nl} \tag{31}$$

$$F = \Gamma^{-1} F_{\text{ext}} \tag{32}$$

On substituting the Fourier approximation of response and its derivatives in the governing equation and subsequent application of Galerkin procedure one can obtain the residual equation given below

$$R = F - \left[J_l^{-1} Q^T + G \right] \tag{33}$$

where R is the residual vector, J_l is the linear Jacobian matrix, F and G are the Fourier coefficient vectors of the external excitation and nonlinear function. Equation (33) is solved using iterative method until Q converges. For every iteration, the Fourier coefficients Q would updated as

$$Q^{i+1} = Q^i - [J_l + J_{nl}]^{-1} R \tag{34}$$

where J_{nl} represents non-linear Jacobian matrix and this will continue a specified tolerance limit $\| R \| < \epsilon$. The converged coefficients will be substituted in Eqs. (24)–(26) to find the response and its derivatives. This method is used to find the periodic solution of snap-through electromagnetic energy harvester in the frequency domain in the subsequent section.

Comparison of analytical and semi-analytical method

Figure 3 shows the frequency response plot of snap-through electromagnetic energy harvester for the following parameters $\zeta = 0.10$, $\alpha = 0.60$, $f = 0.0$, $r = 1.0$, $\theta = 0.40$, $\lambda = 0.80$, and $\mu = 0.30$. The number of harmonics used in theoretical and semi-analytical studies are one. The analytical outcomes are supported by the semi-analytical method is shown in Figure 3.

Bifurcation analysis

The bifurcation analysis is performed in order to understand the global dynamics of the snap-through electromagnetic energy harvester when the system parameters are varied. The bifurcation plots are obtained by numerically integrating Eqs. (3) and (4) equations of motion and then by plotting the Poincare points of the steady state motion for the parameter value. The bifurcation plots are obtained with excitation frequency Ω as parameter for different values of α. The values of other parameters chosen for the studies are $\zeta = 0.015$, $f = 0.10$, $r = 1.0$, $\theta = 0.40$, $\lambda = 0.80$, and $\mu = 0.30$. The different regions of intrawell, interwell and chaotic interwell motions are identified and marked in the bifurcation diagrams as shown in Figure 4(a) and (b). The systems exhibit P1 interwell oscillation for the frequency range $0.80 \le \Omega \le 0.50$ and this behavior is common when α is 0.30 and 0.35. Typical phase plane plots with Poincare points and time history of snap-through energy harvester are shown in Figures 5 and 6.

When α value is 0.40 and 0.45, the period 1 interwell motion frequency range are from $0.85 \le \Omega \le 0.49$ and $0.83 \le \Omega \le 0.40$ respectively as shown in Figure 7(a) and (b). The phase plane plots along with Poincare points and the time

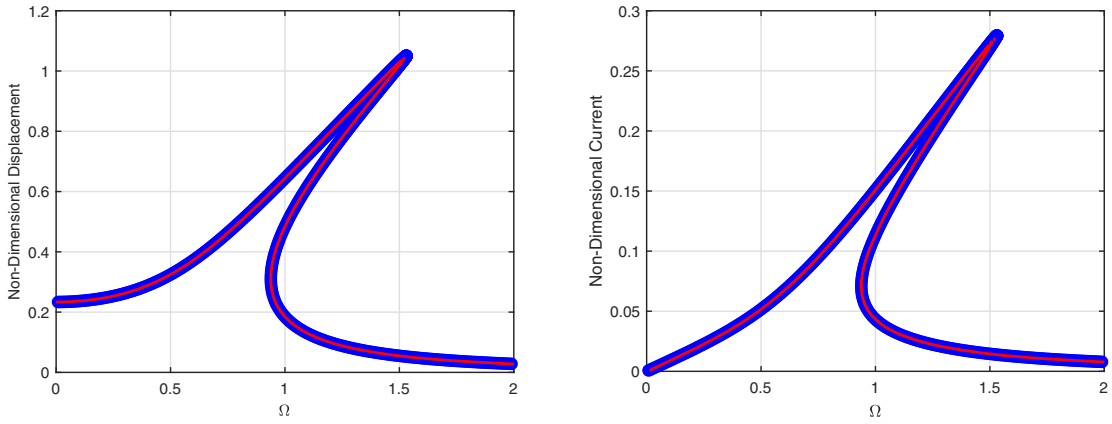

(a) (b)

Figure 3: Comparison of analytical (red line) and semi-analytical (blue line) when $\zeta = 0.10$, $\alpha = 0.60$, $f = 0.10$, $r = 1.0$, $\theta = 0.40$, $\lambda = 0.80$, and $\mu = 0.30$.

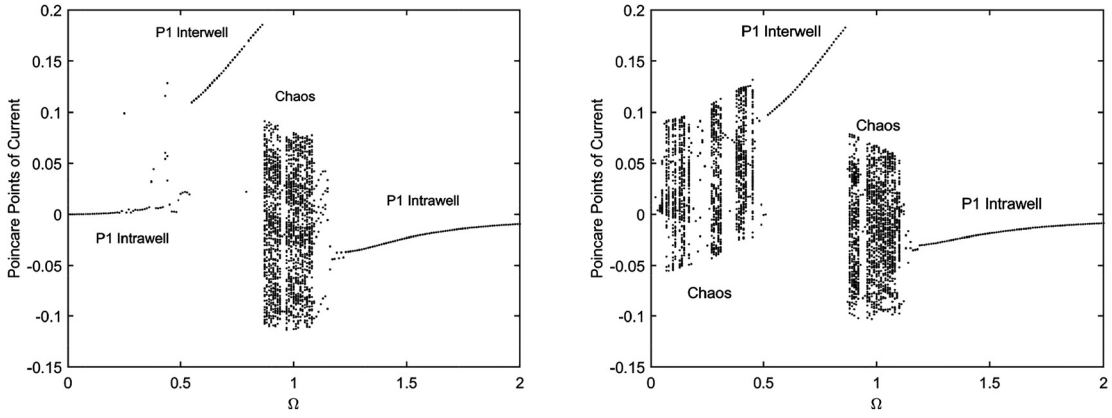

(a) $\alpha = 0.30$ (b) $\alpha = 0.35$

Figure 4: Bifurcation diagram of current response against the excitation frequency Ω when $r = 1.0$, $f = 0.10$, $\zeta = 0.015$, $\theta = 0.40$, $\lambda = 0.80$, and $\mu = 0.30$.

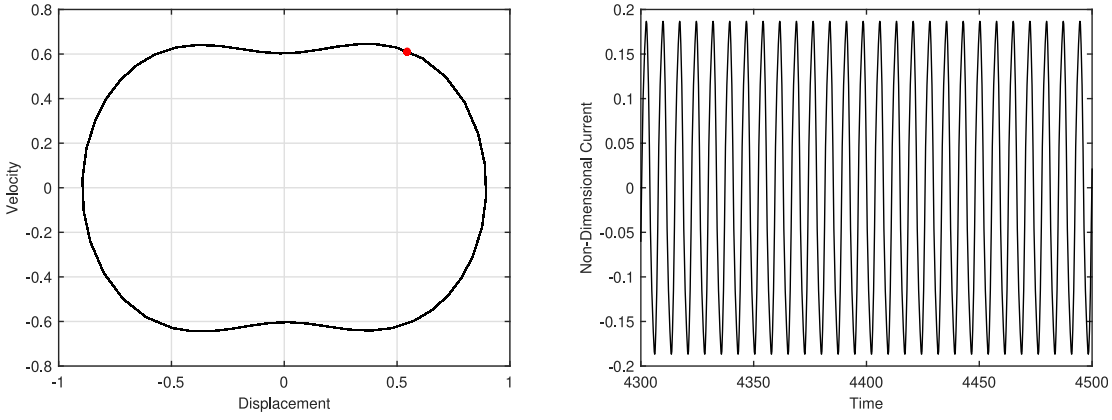

(a) Phase Plane (b) Time Series

Figure 5: Time history and phase portrait diagram of snap-through electromagnetic energy harvester when $\Omega = 0.85$, $r = 1.0$, $f = 0.10$, $\zeta = 0.015$, $\alpha = 0.30$, $\theta = 0.40$, $\lambda = 0.80$ and $\mu = 0.30$.

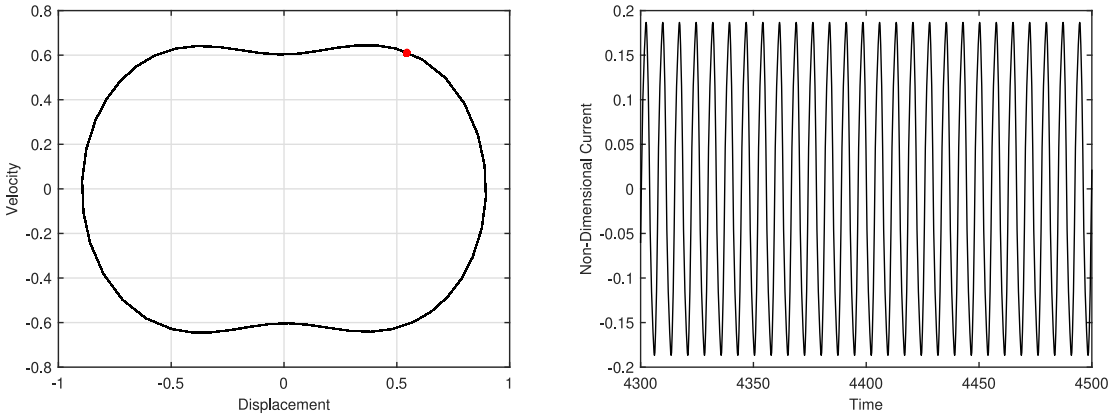

(a) Phase Plane (b) Time Series

Figure 6: Time history and phase portrait diagram of snap-through electromagnetic energy harvester when $\Omega = 0.85$, $r = 1.0$, $f = 0.10$, $\zeta = 0.015$, $\alpha = 0.35$, $\theta = 0.40$, $\lambda = 0.80$ and $\mu = 0.30$.

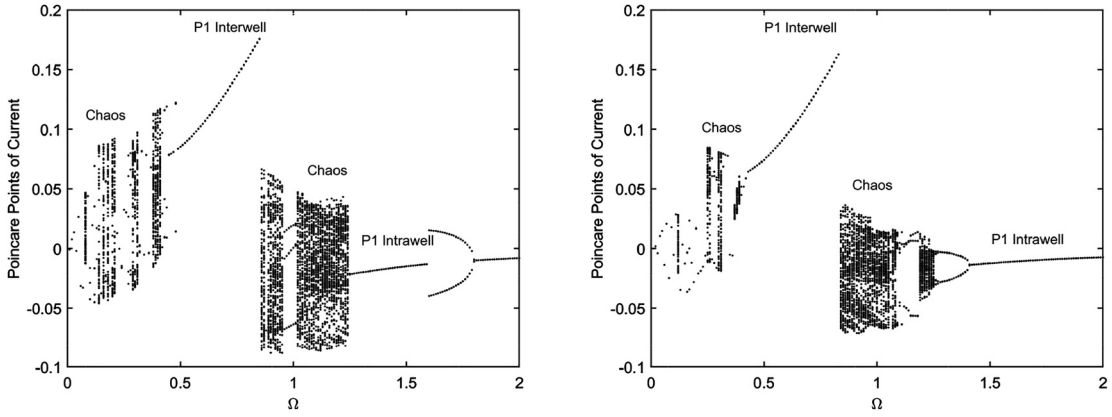

(a) $\alpha = 0.40$ (b) $\alpha = 0.45$

Figure 7: Bifurcation diagram of current response against the excitation frequency Ω when $r = 1.0$, $f = 0.10$, $\zeta = 0.015$, $\theta = 0.40$, $\lambda = 0.80$, and $\mu = 0.30$.

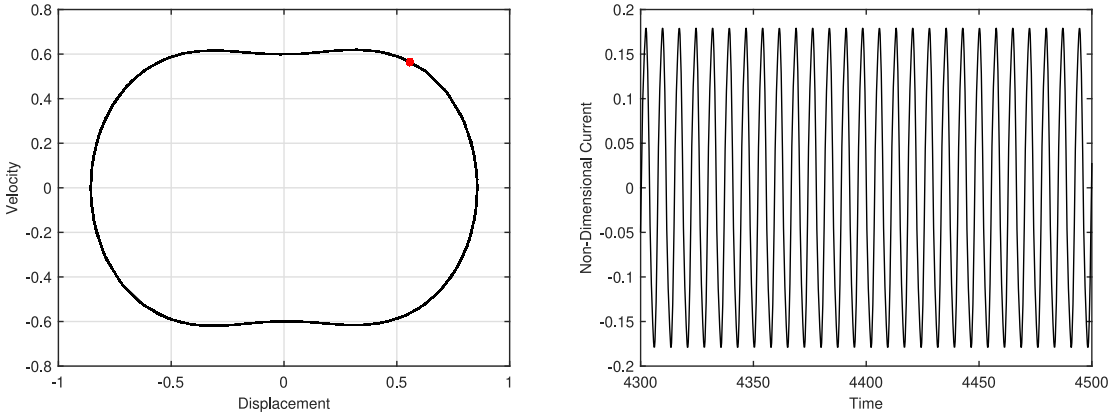

(a) Phase Plane (b) Time Series

Figure 8: Time history and phase portrait diagram of snap-through electromagnetic energy harvester when $\Omega = 0.85$, $r = 1.0$, $f = 0.10$, $\zeta = 0.015$, $\alpha = 0.40$, $\theta = 0.40$, $\lambda = 0.80$ and $\mu = 0.30$.

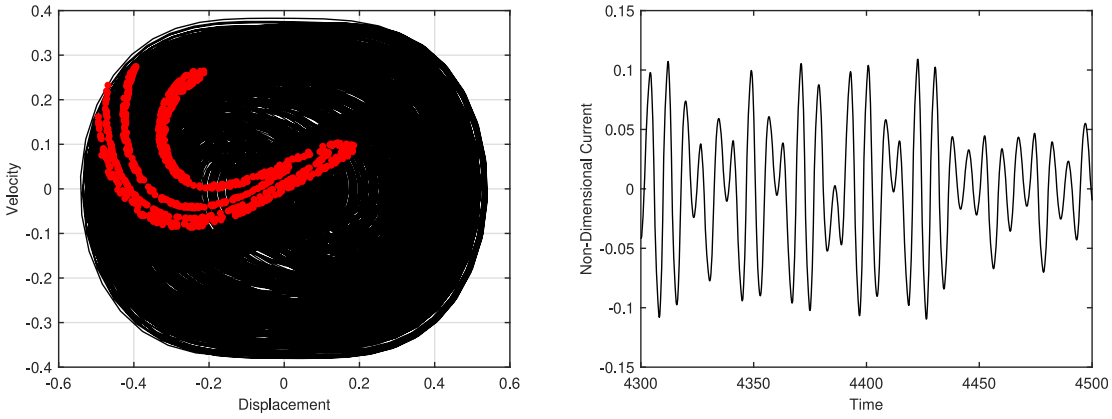

(a) Phase Plane (b) Time Series

Figure 9: Time history and phase portrait diagram of snap-through electromagnetic energy harvester when $\Omega = 0.85$, $r = 1.0$, $f = 0.10$, $\zeta = 0.015$, $\alpha = 0.45$, $\theta = 0.40$, $\lambda = 0.80$ and $\mu = 0.30$.

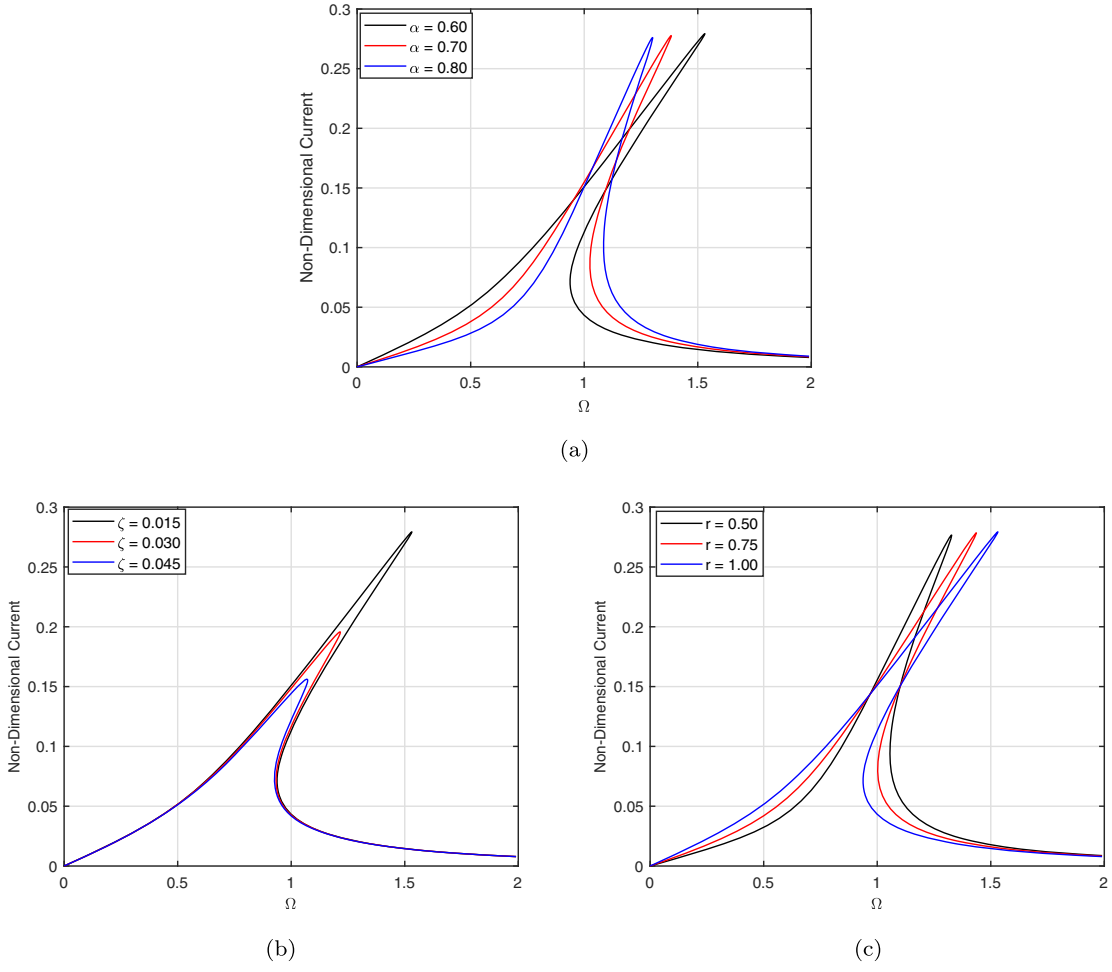

(a)

(b) (c)

Figure 10: Effect of mechanical parameters ζ, r and α on the response of the snap-through electromagnetic energy harvester when $f = 0.10$, $\theta = 0.40$, $\lambda = 0.80$ and $\mu = 0.30$ and other parameters (a) $\zeta = 0.015$, $r = 1.0$ (b) $\alpha = 0.60$, $r = 1.0$ (c) $\zeta = 0.015$, $\alpha = 0.60$.

histories for $\alpha = 0.40$ and 0.45 are shown in Figure 8(a) and (b). It is observed chaotic motion with strange attractor appeared as shown in Figure 9(a).

Parametric study

In this section, a parametric study is performed on the system given by Eqs. (9) and (10) using MHBM. The frequency response of the system is generated for different system parameter values for snap-through electromagnetic energy harvester. Frequency response for the snap-through energy harvester are obtained for α = 0.60, 0.70 and 0.80 are shown in Figure 10a. When $\alpha = 0.60$, the system shows a hardening behavior with an associated jump phenomenon and when α increases, the hardening behavior tends to softening behavior and vice versa when r value increases as shown in Figure 10c. Finally, when the damping ratio increases, the amplitude of the harvested current is reducing as shown in Figure 10b.

As observed from the response plots, for the selected parameters, the snap-through electromagnetic energy harvester are not much sensitive to the change in the values of λ as shown in Figure 11c. When the electromechanical coupling coefficient θ increases, the nonlinear effect become more prominent. The frequency response curve bends towards the right and multiple solution regions can be observed as shown in Figure 11b. For higher values of θ, the non-dimensional current of the system is comparatively smaller and the nonlinear effects are not prominent. When μ is increases, curves bends towards right and the hardening behavior is increases as shown in Figure 11a. Important conclusions can be arrived from the parametric study conducted in this section. The response of the snap-through electromagnetic energy harvester are sensitive to parameter changes of system. The performance of the system can be increased by selecting proper system parameters.

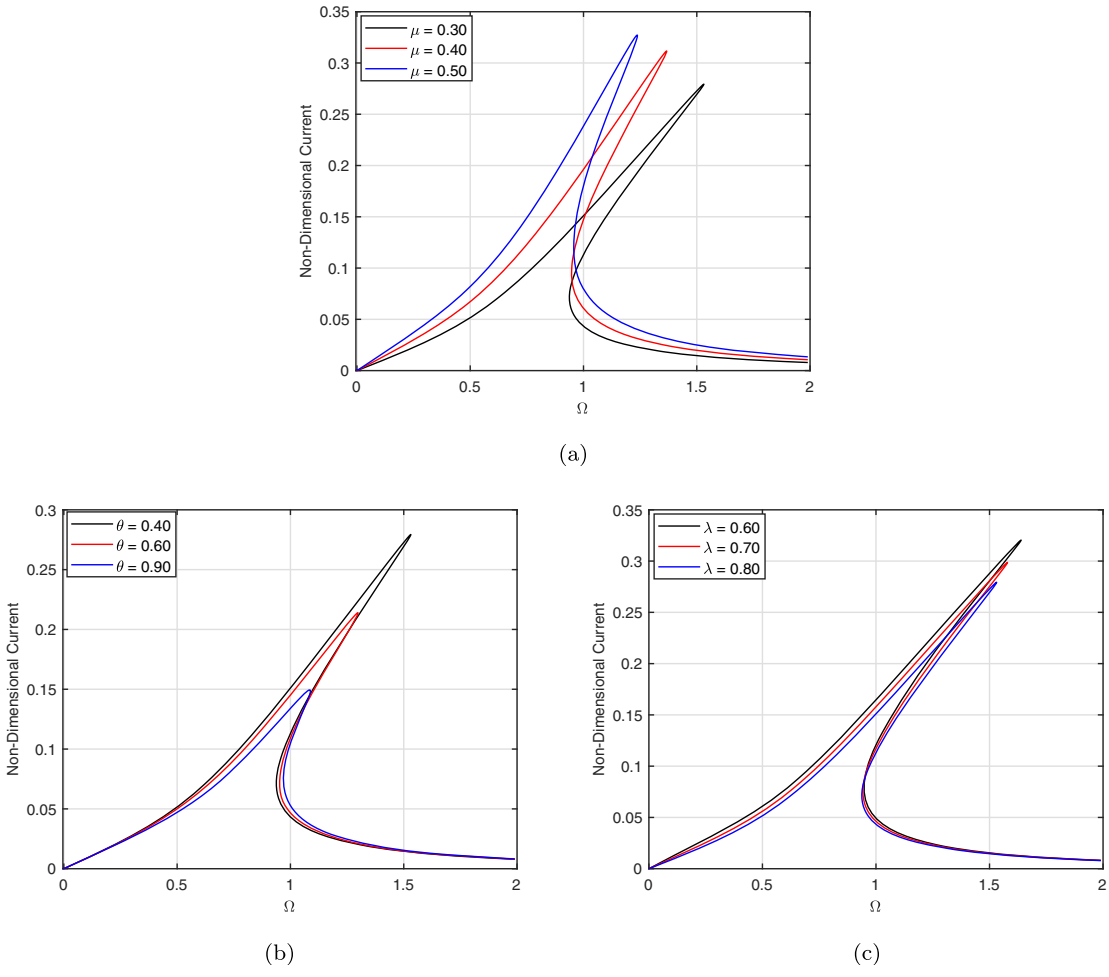

Figure 11: Influence of electrical parameters μ, θ and λ on the response of the snap-through electromagnetic energy harvester when $f = 0.10$, $\zeta = 0.015$, $r = 1.00$ and $\alpha = 0.60$ and other parameters (a) $\theta = 0.40$, $\lambda = 0.80$ (b) $\mu = 0.30$, $\lambda = 0.80$ (c) $\mu = 0.30$, $\theta = 0.40$.

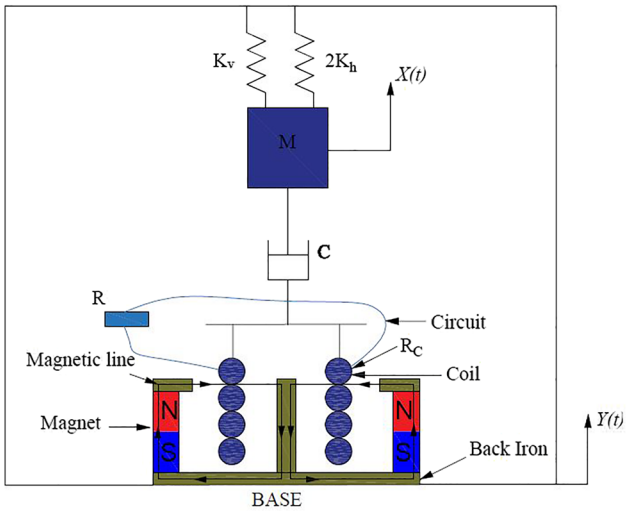

Figure 12: Linear stiffness system of similar size with electromagnetic transduction mechanism.

Performance comparisons

In this section, the energy harvesting performances of the snap-through electromagnetic energy harvester and the linear electromagnetic energy harvester are compared using MHBM. The performance is measured by the steady state current response produced by the system. To demonstrate the benefits of using a snap-through energy harvester relative to a linear energy harvester, a linear electromagnetic energy harvester is built as shown in Figure 12. The size of the harvester is the key issue in the design, and the size is mainly decided by the static equilibrium positions. In this design, the linear and the nonlinear systems have the same static equilibrium position so that the linear and the nonlinear harvesters are in the similar size. Figure 12 shows a design of a linear electromagnetic energy harvester.

The non-dimensional governing equations of linear electromagnetic energy harvester are

$$x'' + 2\zeta x' + (1+r)x + \theta I = f\cos(\Omega\tau) \tag{35}$$

$$I' + \lambda I - \mu x' = 0 \tag{36}$$

In the simulations, the system parameters are selected as $\zeta = 0.015, f = 0.10, r = 1.0, f = 0.10, \theta = 0.40, \lambda = 0.80, \mu = 0.30$ and $\alpha = 0.60$ for snap-through harvester. Figure 13 shows that the performance of the snap-through electromagnetic energy harvester is better than that of the linear system in the similar size for wider range of excitation frequency.

Parameter optimization

In this section, optimization is performed to find the system parameter values that will maximize the energy harvesting performance of snap-through electromagnetic energy harvester. Raj and Santhosh (2019) proposed a methodology to find the optimal parameters for both vibration absorption and energy harvesting, and the same has been adapted in this work. In this study, six factors and three levels are considered and the optimization procedure is performed for the following parameters: ζ, r, α, μ, λ and θ. The objective function can be converted into maximization problem and is given by

$$f = \max[I(\alpha, \zeta, r, \mu, \theta, \lambda)] \tag{37}$$

The range of constraints are selected with respect to the parametric study conducted in the previous section and they are $0.60 \le \alpha \le 0.80$, $0.015 \le \zeta \le 0.045$, $0.50 \le r \le 1.0$,

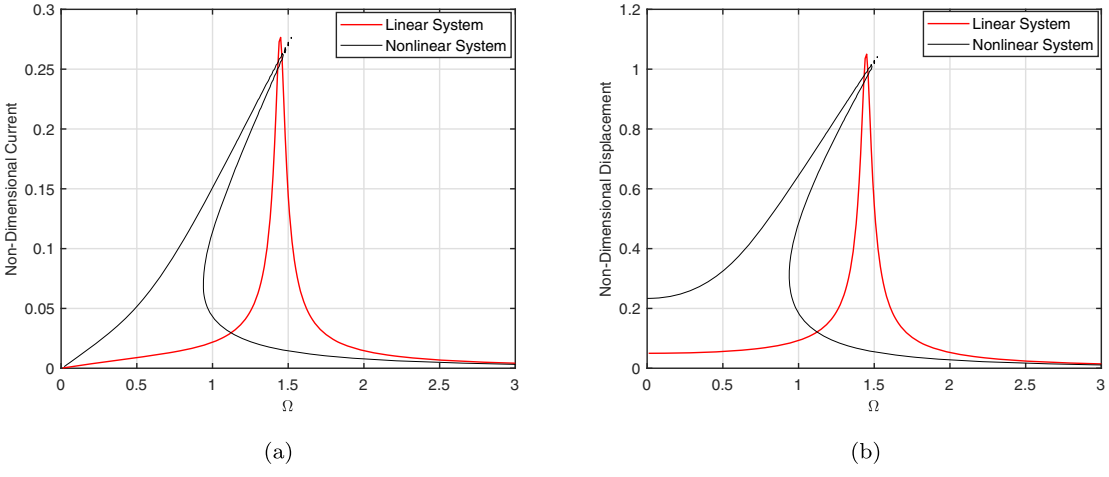

Figure 13: The performance comparison of snap-through electromagnetic energy harvester with $\alpha = 0.60$ and linear electromagnetic energy harvester in the similar size when $\zeta = 0.015$, $f = 0.10$, $r = 1.0$, $\theta = 0.40$, $\lambda = 0.80$ and $\mu = 0.30$.

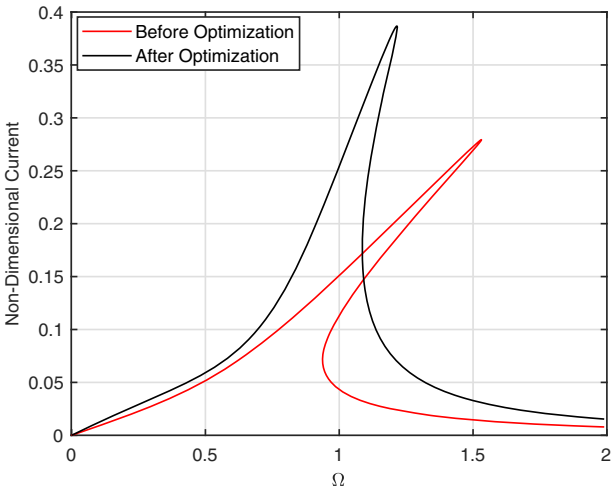

Figure 14: Comparison of non-dimensional current for initial and optimized parameter values of snap-through electromagnetic vibration energy harvester when $f = 0.10$.

$0.30 \le \mu \le 0.50$, $0.40 \le \theta \le 0.90$, $0.60 \le \lambda \le 0.80$. The optimum parameter value of the maximizing the energy harvesting capabilities of snap-through electromagnetic vibration energy harvester are obtained as $\alpha = 0.60$, $\zeta = 0.015$, $r = 0.501$, $\mu = 0.499$, $\theta = 0.40$ and $\lambda = 0.60$. The comparison of non-dimensional current for the initial parameter values mentioned in Figure 3b and for the optimized values are shown in Figure 14. The optimized parameter results in an increases in current and thus results in an increase in harvester power.

Conclusion

This paper presents a theoretical and semi-analytical MHBM framework to analyze and predict the steady state responses of a base excited snap-through electromagnetic energy harvester. The approximate solutions are obtained by using analytical and semi-analytical method. The analytical solution is obtained by theoretical harmonic balance method is compared with semi-analytical MHBM. Bifurcation diagrams obtained with excitation frequency as parameters show the existence of periodic interwell, intrawell and chaotic solutions. Parametric study demonstrate that the non-dimensional geometric coefficient, ratio of stiffness and the electromechanical coupling coefficient plays a significant roles for the energy harvesting performance. The snap-through is a promising nonlinearity mechanism to improve energy harvesting and the snap-through electromagnetic energy harvester outperforms the similar size linear energy harvester under harmonic excitation. An optimization problem based on genetic algorithm is formulated for the purpose of optimizing parameters and optimized values of parameters which enhanced the current that can be harvested from the system.

Author contributions: The author has accepted responsibility for the entire content of this submitted manuscript and approved submission.
Research funding: None declared.
Conflict of interest statement: The author declares no conflicts of interest regarding this article.

References

Ali, S.F., and S. Adhikari. 2013. "Energy Harvesting Dynamic Vibration Absorbers." *Journal of Applied Mechanics* 80 (4): 041004–9.
Cao, Q., M. Wiercigroch, E. E. Pavlovskaia, C. Grebogi, and J. M. T. Thompson. 2006. "Archetypal Oscillator for Smooth and Discontinuous Dynamics." *Physical Review E* 74 (4): 046218.
Cao, Q., M. Wiercigroch, E. E. Pavlovskaia, C. Grebogia, and J. M. T. Thompson. 2008. "The Limit Case Response of the Archetypal Oscillator for Smooth and Discontinuous Dynamics." *International Journal of Non-Linear Mechanics* 43 (6): 462–73.
Daqaq, M. F., R. Masana, A. Erturk, and D. Dane Quinn. 2014. "On the Role of Nonlinearities in Vibratory Energy Harvesting: A Critical Review and Discussion." *Applied Mechanics Reviews* 66 (4): 040801.
Elvin, N., and A. Erturk. 2013. *Advances in Energy Harvesting Methods*. New York: Springer Science.
Erturk, A., and D. J. Inman. 2011. *Piezoelectric Energy Harvesting*. UK: John Wiley and Sons Ltd, Wiley.
Erturk, A., and D. J. Inman. 2011. "Broadband Piezoelectric Power Generation on High-Energy Orbits of the Bistable Duffing Oscillator with Electro Mechanical Coupling." *Journal of Sound and Vibration* 330 (10): 2339–53.
Harne, R. L., and K. W. Wang. 2013. "A Review of the Recent Research on Vibration Energy Harvesting via Bistable Systems." *Smart Materials and Structures* 22 (2): 023001.
Harne, R. L., and W. Kon-Well. 2017. *Harnessing Bistable Structural Dynamics: For Vibration Control, Energy Harvesting and Sensing*. UK: John Wiley & Sons Ltd.
Jiang, W.-A., and L.-Q. Chen. 2014. "Snap-Through Piezoelectric Energy Harvesting." *Journal of Sound and Vibration* 333 (18): 4314–25.
Jiang, W.-A., and L.-Q. Chen. 2016. "Stochastic Averaging of Energy Harvesting Systems." *International Journal of Non-Linear Mechanics* 85: 174–87.
Priya, S., and D. J. Inman. 2009. *Energy Harvesting Technologies*. USA: Springer.
Raj, R., and B. Santhosh. 2019. "Parametric Study and Optimization of Linear and Nonlinear Vibration Absorbers Combined with Piezoelectric Energy Harvester." *International Journal of Mechanical Sciences* 152: 268–79.
Raj, R., and B. Santhosh. 2020. "A Comparative Study on the Primary System Response and Energy Harvesting from Linear and Nonlinear Tuned Vibration Absorbers." In *Advances in Rotor*

Dynamics, Control, and Structural Health Monitoring, edited by S. Dutta, E. Inann, and S. K. Dwivedy, 429–40. Springer Singapore.

Ramlan, R., M. J. Brennan, B. R. Mace, and I. Kovacic. 2010. "Potential Benefits of a Nonlinear Stiffness in an Energy Harvesting Device." *Nonlinear Dynamics* 59 (4): 545–58.

Rantz, R., and S. Roundy. 2017. "Characterization of Real-World Vibration Sources and Application to Nonlinear Vibration Energy Harvesters." *Energy Harvesting and Systems* 4 (2): 67–76.

Santhosh, B., and A. S. Das. 2016. "Energy Harvesting from Nonlinear Vibration Absorbers." *Procedia Engineering* 144: 653–9.

Santhosh, B., C. Padmanabhan, and S. Narayanan. 2014. "Numeric-analytic Solutions of the Smooth and Discontinuous Oscillator." *International Journal of Mechanical Sciences* 84: 102–19.

Tian, R., Q. Cao, and S. Yang. 2010. "The Codimension-Two Bifurcation for the Recent Proposed Sd Oscillator." *Nonlinear Dynamics* 59 (1): 19–27.

Tran, N., M. H. Ghayesh, and M. Arjomandi. 2018. "Ambient Vibration Energy Harvesters: A Review on Nonlinear Techniques for Performance Enhancement." *International Journal of Engineering Science* 127: 162–85.

Yang, T., and Q. Cao. 2020. "Dynamics and High-Efficiency of a Novel Multi-Stable Energy Harvesting System." *Chaos, Solitons & Fractals* 131: 109516.

Yang, T., J. Liu, and Q. Cao. 2018. "Response Analysis of the Archetypal Smooth and Discontinuous Oscillator for Vibration Energy Harvesting." *Physica A: Statistical Mechanics and its Applications* 507: 358–73.

Yildirim, T., M. H. Ghayesh, W. Li, and G. Alici. 2017. "A Review on Performance Enhancement Techniques for Ambient Vibration Energy Harvesters." *Renewable and Sustainable Energy Reviews* 71: 435–49.

Zhou, Y., R. Varghese, A. Chopra, K. Sang-Gook, I. Kanno, L. Wu Dong, S. Ha, J. Ryu, S. Priya, S. Hyun-Cheol, and R. G. Polcawich. 2017. "A Review on Piezoelectric Energy Harvesting: Materials, Methods, and Circuits." *Energy Harvesting and Systems* 4 (1): 3–39.